IOPscience iopscience.iop.org

Home Search Collections Journals About Contact us My IOPscience

Vibrational study of phase transitions in $K_3Nb_3O_6(BO_3)_2$ crystal

This article has been downloaded from IOPscience. Please scroll down to see the full text article.

2005 J. Phys.: Condens. Matter 17 3355

(http://iopscience.iop.org/0953-8984/17/21/028)

View the table of contents for this issue, or go to the journal homepage for more

Download details:
IP Address: 129.252.86.83
The article was downloaded on 28/05/2010 at 04:54

Please note that terms and conditions apply.

INSTITUTE OF PHYSICS PUBLISHING JOURNAL OF PHYSICS: CONDENSED MATTER

J. Phys.: Condens. Matter **17** (2005) 3355–3366 doi:10.1088/0953-8984/17/21/028

Vibrational study of phase transitions in $K_3Nb_3O_6(BO_3)_2$ crystal

M Mączka[1], K Hermanowicz[1] and J Hanuza[1,2]

[1] Institute of Low Temperature and Structure Research, Polish Academy of Sciences, PO Box 1410, 50-950 Wrocław 2, Poland
[2] Department of Bioorganic Chemistry, Faculty of Industry and Economics, Wrocław University of Economics, 118/120 Komandorska Street, 53-345 Wrocław, Poland

Received 1 February 2005, in final form 7 April 2005
Published 13 May 2005
Online at stacks.iop.org/JPhysCM/17/3355

Abstract

The temperature dependences of Raman- and IR-active phonons of $K_3Nb_3O_6(BO_3)_2$ are reported, for probing the two ferroelectric–ferroelastic phase transitions. The phonon frequencies are found to change discontinuously near 185 ± 5 and 385 ± 5 K. The character of the observed changes shows that the transitions lead to significant changes in the NbO_6 octahedra. The results obtained show also that many low frequency modes exhibit hardening upon heating. Moreover, at high temperatures the damping of some modes increases significantly. The origin of this behaviour is discussed.

1. Introduction

Among the known crystalline materials in nonlinear optics, boron containing compounds play an important role since these materials usually have rather high $\chi^{(2)}$ and $\chi^{(3)}$ nonlinear susceptibilities [1]. Moreover, borates have a cut-off wavelength in the near-ultraviolet region and have outstanding resistance to laser damage [1–4]. $K_3Nb_3O_6(BO_3)_2$ is a promising nonlinear borate. It has been shown that this borate exhibits a number of ferroelastic and ferroelectric phase transitions below 783 K [5–8]. Dielectric and ionic conductivity studies showed that this material also exhibits superionic properties [7, 8]. Recently, $K_3Nb_3O_6(BO_3)_2$ has also been found to be an attractive $\chi^{(3)}$-active crystal for picosecond stimulated Raman scattering generation in the visible and near-IR region [9].

In the present paper we report the temperature dependences of Raman-and IR-active phonons in the 8–540 K range, obtained in order to get some insight into the mechanism of two phase transitions occurring near 185 and 385 K. Our studies show that these transitions are discontinuous. They are associated with weak modification of the local environment of the Nb atoms within their oxygen octahedra, as well as the local environment of the K^+ ions. Our results suggest also that this material exhibits another, possibly second-order phase transition near 80 K, which has not yet been reported.

 © 2005 IOP Publishing Ltd Printed in the UK

2. Experiment

The $K_3Nb_3O_6(BO_3)_2$ crystals were grown from the flux. The mixture of K_2CO_3, Nb_2O_5, and B_2O_3, corresponding to the composition $K_3Nb_3O_6(BO_3)_2$ and $K_2B_4O_7$ in a ratio 1:1, was placed in a platinum crucible, heated to 1000 °C, kept at this temperature for 40 h, cooled at a rate of 2 °C to 840 °C, and then cooled at a rate 10 °C to room temperature. The crystals obtained were extracted from the crucible by washing with hot water. Single crystals had the form of hexagonal rods up to 5 mm in length and up to 2 × 2 mm in cross-section.

Because the crystals obtained were too small for single-crystal transmission or reflection studies, only polycrystalline infrared spectra were measured from the ground crystals with a Biorad 575C FT-IR spectrometer, in KBr suspension for the 1500–400 cm^{-1} region and in Nujol suspension for the 500–30 cm^{-1} region. FT Raman spectra were measured for an oriented single crystal using a BRUKER 110/S spectrometer with the YAG:Nd^{3+} excitation. Temperature-dependent studies of IR and Raman spectra below 300 K temperature were performed using a helium-flow Oxford cryostat. Temperature-dependent Raman spectra in the 300–540 K region were measured using in a Linkam cryostat cell (THMS 600). Both IR and Raman spectra were recorded with a spectral resolution of 2 cm^{-1}.

3. Results and discussion

3.1. Selection rules and assignments of vibrational modes

The high temperature, prototype structure of $K_3Nb_3O_6(BO_3)_2$ is hexagonal, with space group $P\bar{6}2m$, and is isomorphous with the room temperature structure of $K_3Ta_3O_6(BO_3)_2$ [10]. This structure contains one molecule in the unit cell and it is build up of triple groups of NbO_6 octahedra linked by planar BO_3^{3-} triangles. The three-dimensional structure composed of BO_3^{3-} triangles and NbO_6 octahedra contains large pentagonal cavities occupied by K^+ ions [10]. At room temperature the structure is slightly distorted and the structure can be described as orthorhombic, with space group $P2_1ma$ [11]. The unit cell of this modification contains four formula units. The comparison of the high and room temperature modifications shows that the hexagonal–orthorhombic distortion is only 0.01 % at room temperature [11].

The factor group analysis predicts that there should be $6A_1' + 6A_2' + 2A_1'' + 6A_2'' + 14E' + 6E''$ ($64A_1 + 56A_2 + 56B_1 + 64B_2$) vibrational modes for the $P\bar{6}2m$ ($P2_1ma$) structure (the modes given in parentheses correspond to the orthorhombic structure). These modes can be subdivided into $A_1' + A_2' + A_1'' + A_2'' + 4E'$ ($12A_1 + 12A_2 + 12B_1 + 12B_2$) internal modes of the BO_3^{-3} ions, $A_1'' + A_2'' + 2E'$ ($6A_1 + 6A_2 + 6B_1 + 6B_2$) translational motions of BO_3^{3-} groups, $A_1' + A_2' + 2E''$ ($6A_1 + 6A_2 + 6B_1 + 6B_2$) librational modes of the BO_3^{3-}, $A_1' + A_2' + A_2'' + 2E' + E''$ ($10A_1 + 8A_2 + 8B_1 + 10B_2$) translational motions of K^+ ions, $A_1' + A_2' + A_2'' + 2E' + E''$ ($10A_1 + 8A_2 + 8B_1 + 10B_2$) translational motions of Nb^{6+} ions, $A_1' + A_2' + A_2'' + E' + E''$ ($8A_1 + 4A_2 + 8B_1 + 8B_2$) stretching modes of the NbO_6 octahedra, and $A_1' + A_2' + A_2'' + 3E' + E''$ ($12A_1 + 12A_2 + 8B_1 + 12B_2$) bending and librational modes of the NbO_6 octahedra. It should be noticed, however, that the $E' + A_2''$ (A_1, B_1, B_2) acoustic modes should be subtracted from the translational modes. The A_1' and E'' (A_2) modes are Raman-active, A_2'' modes are IR-active, E' (A_1, B_1, B_2) modes are both Raman- and IR-active, and A_2' and A_1'' modes are inactive in vibrational spectroscopy.

The recorded spectra are presented in figures 1 and 2. At room temperature a total of 23 Raman and 17 IR bands were observed. This number is close to the number of Raman and IR modes predicted for the hexagonal phase (26 and 20, respectively), which confirms the small orthorhombic distortion of the parent hexagonal phase. Former studies of a number of borates showed that the symmetric stretching (ν_1), asymmetric stretching (ν_3), out-of-plane

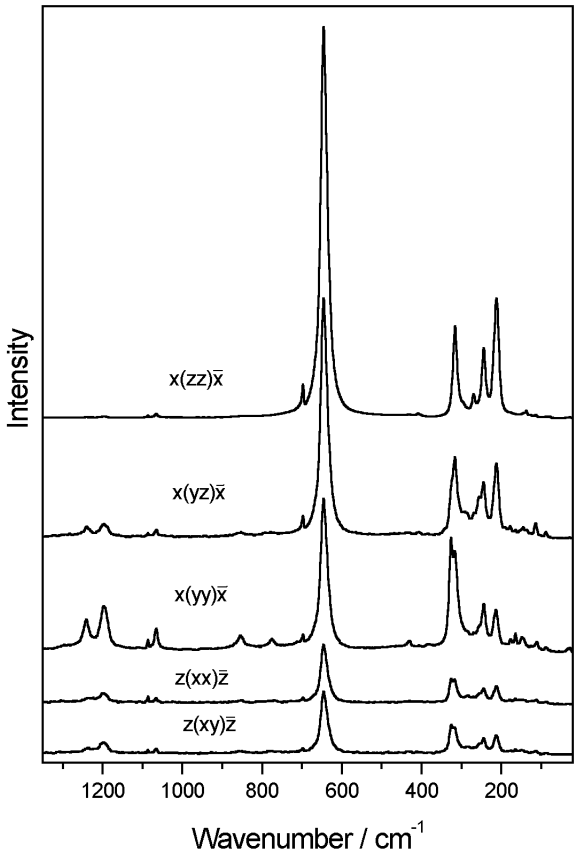

Figure 1. Room temperature Raman spectra of $K_3Nb_3O_6(BO_3)_2$ for a few polarization configurations. The notation refers to hexagonal symmetry. The spectrum for the $x(zz)x$ polarization is very intense and was, therefore, divided by 5 to ease comparison with the other spectra.

bending (ν_2), and in-plane bending (ν_4) modes of the BO_3^{3-} units are observed around 950–1050, 1250–1400, 670–800, and 600–660 cm^{-1}, respectively [4, 12–15]. According to the correlation diagram, presented in table 1, for the hexagonal phase two components of the ν_3 modes should be observed both in IR and Raman spectra whereas only one ν_1 component is predicted to be Raman-active. In the orthorhombic structure the ν_1 and ν_3 modes should split into 8 Raman (6 IR) and 16 Raman (12 IR) components, respectively (see table 1). Our spectra show, however, that even at room temperature only one ν_1 mode at 1066 cm^{-1} and two ν_3 modes near 1200–1300 cm^{-1} are observed (see figures 1 and 2, and table 2). This observation confirms the small deviation of this phase from its parent hexagonal symmetry. The ν_2 mode can be unambiguously located near 780 cm^{-1}. The $\nu_4(BO_3)$ mode could be attributed to the strong IR bands observed at 631 and 625 cm^{-1}. However, the former studies of borates showed that this mode is usually observed as a relatively weak IR band [12, 15, 16]. Moreover, the studies of niobates and tungstates showed that these materials give a very strong IR band near 600 cm^{-1} which can be assigned to the antisymmetric stretching mode of NbO_6 (WO_6) octahedra [16, 17]. We assign, therefore, the very intense IR band at 631 cm^{-1} with a shoulder at 625 cm^{-1} to the $\nu_4(BO_3)$ modes and antisymmetric stretching mode of the NbO_6 octahedra.

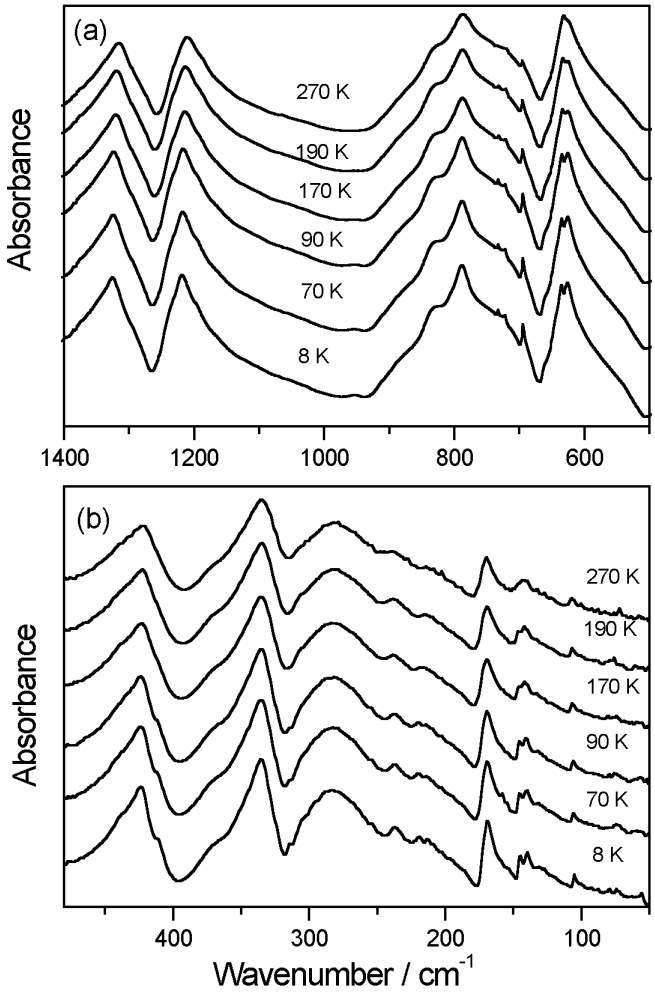

Figure 2. Temperature dependence of polycrystalline IR spectra of $K_3Nb_3O_6(BO_3)_2$ in the mid-IR (a) and far-IR (b) regions.

The studies of niobates showed also that NbO_6 groups should show the presence of a very strong Raman mode due to symmetric stretching vibration of NbO_6 groups. This mode was usually observed around 600–650 cm^{-1} [17–20]. We assign to this mode the strongest Raman band observed at 647 cm^{-1}. The very weak Raman band at 857 cm^{-1} has most likely the same origin as the 868 and 834 cm^{-1} bands observed for $NaNbO_3$ and $KNbO_3$, respectively [18, 19]. The assignment of this band is not clear since it is assigned either as the LO component of the strongest Raman line or as a combination mode [18, 19]. Our IR and Raman spectra show also the presence of a very narrow band at 699 cm^{-1}. The origin of this band is not known.

The former studies of borates showed that $T'(BO_3)$ and $L(BO_3)$ modes are observed in the 280–500 and 150–250 cm^{-1} regions, respectively, as weak Raman bands [13–16, 21]. On the other hand, bending and librational vibrations of niobates were shown to give rise to intense Raman and IR bands in the 300–150 cm^{-1} region [18–20]. Because many modes in the low frequency region have similar energy, we may expect to observe strong couplings between the

Table 1. The correlation diagram showing the correspondence between the optical modes of the free BO_3^{3-} ion and the modes in the $P\bar{6}2m$ (upper part) and $P2_1ma$ structure (lower part) of $K_3Nb_3O_6(BO_3)_2$.

	Symmetry of BO_3^{3-} ion	Site symmetry	Factor group symmetry
	D_{3h}	C_{3h}	D_{3h}
ν_1	A_1'(RS)	A'(RS)	A_1'(RS) + A_2'(iA)[a]
ν_2	A_2''(IR)	A''(IR)	A_1''(iA) + A_2''(IR)
ν_3, ν_4	E'(IR, RS)	E'(IR, RS)	$2E'$(IR, RS)
	D_{3h}	C_1	C_{2v}
ν_1	A_1'(RS)	A(IR, RS)	$2A_1$(IR, RS) + $2A_2$(RS) + $2B_1$(IR, RS) + $2B_2$(IR, RS)
ν_2	A_2''(IR)	A(IR, RS)	$2A_1$(IR, RS) + $2A_2$(RS) + $2B_1$(IR, RS) + $2B_2$(IR, RS)
ν_3, ν_4	E'(IR, RS)	2A(IR, RS)	$4A_1$(IR, RS) + $4A_2$(RS) + $4B_1$(IR, RS) + $4B_2$(IR, RS)

[a] iA denotes inactive modes.

Table 2. Energy of room temperature Raman and IR modes in cm^{-1} for $K_3Nb_3O_6(BO_3)_2$ crystal. s, sh, m, w, vs, and vw denote strong, shoulder, medium, weak, very strong, and very weak, respectively.

Raman					
$x(yy)x$	$x(zz)x$	$x(yz)x$	$z(xy)z$	IR	Assignment
1240w	1238vw	1239w	1238w	1313s	$\nu_3(BO_3)$
1198w	1199vw	1197w	1198w	1208s	$\nu_3(BO_3)$
1066w	1066vw	1067w	1066w	—	$\nu_1(BO_3)$
857w	857vw	857vw	854vw	826sh	?
780w	—	779vw	779vw	786s	$\nu_2(BO_3)$
699w	699w	699w	699vw	695vw	?
647s	647vs	647s	647s	—	$\nu(NbO_6)$
637m	639m	638m	637m	631s	$\nu(NbO_6) + \nu_4(BO_3)$
—	—	—	—	625sh	$\nu(NbO_6) + \nu_4(BO_3)$
432vw	—	—	—	424s	
—	—	—	—	368sh	
327m	326sh	327sh	326m	337s	
317m	317m	317m	316m	—	
289w	287w	289vw	288vw	286s	$T'(BO_3)$, $L(BO_3)$,
270vw	270w	270w	269vw	—	$\delta(NbO_6)$ and $L(NbO_6)$
257w	256sh	256sh	255w	—	
244m	245m	244m	244m	240w	
221sh	216sh	216sh	218sh	215w	
212m	210m	210m	212m	—	
177w	178vw	178vw	176vw	171m	
164w	167vw	164vw	164w	—	
156	—	—	—	—	
150sh	—	—	149w	147sh	$T'(Nb^{6+})$ and
143w	144vw	145vw	145vw	144w	$T'(K^+)$
137sh	138vw	138vw	137vw	—	
112w	113w	113w	113w	108vw	
89vw	—	89vw	88vw	—	

different bending, translational, and librational vibrations of the same symmetry. We, therefore, assign the bands observed in the 200–430 cm^{-1} region to the modes involving complicated

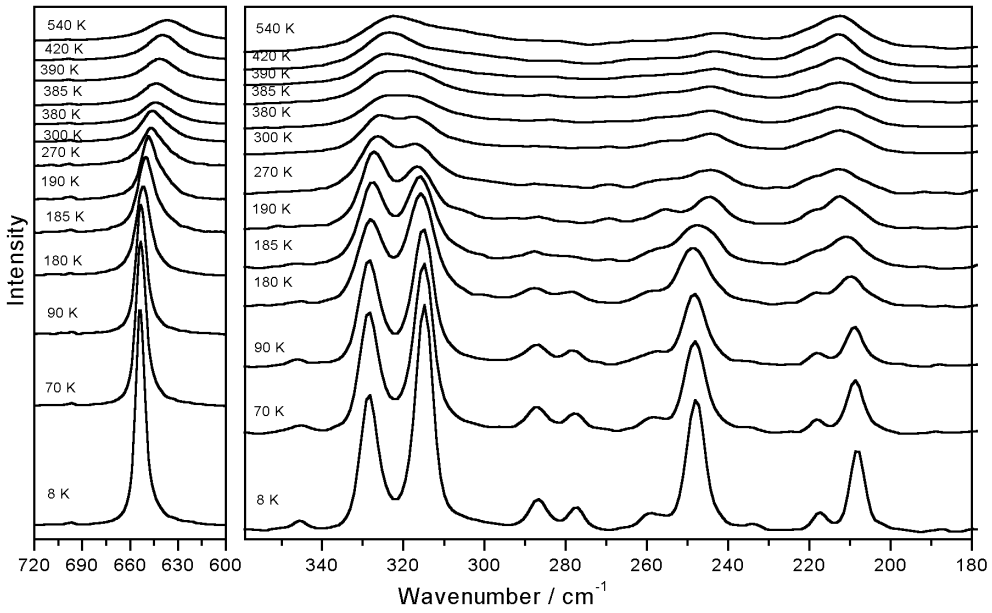

Figure 3. Temperature dependence of the most characteristic Raman modes of $K_3Nb_3O_6(BO_3)_2$ measured in the polarization $x(yy)x$.

bending and librational motions of the niobate groups as well as librational and translational motions of the borate ions. The studies of niobates showed also that translations of alkali metal and niobium ions give significant contributions to modes observed below 220 cm^{-1} [19, 20, 22]. We, therefore, assign the number of very weak Raman bands below 200 cm^{-1} and all IR bands below 220 cm^{-1} to translational motions of Nb^{6+} and K^+ ions.

3.2. Temperature dependence of IR and Raman modes of $K_3Nb_3O_6(BO_3)_2$

Typical Raman spectra of $K_3Nb_3O_6(BO_3)_2$ at various temperatures on cooling, for $x(yy)x$ and $x(zz)x$ polarization configurations, are shown in figures 3 and 4. During cooling, the Raman spectra remain almost the same down to 390 K. When the temperature reaches 385 K, a series of evident changes take place. We observe large changes in relative intensity of some bands and some changes in frequencies of observed bands (see figures 3 and 4 and discussion below). This modification indicates the first structural phase transition. Further changes, indicative of the onset of another phase transition, occur at about 185 K. It is observed that some modes upshift or downshift, along with changes in their relative intensity. During cooling below 185 K no significant changes in frequency of modes are observed. However, we observe at 80 K an abrupt intensity change of some modes for the $y(xz)y$ polarization. This change is very clearly observed in figure 5, which shows the temperature dependence of the depolarization ratio $\rho = I_{yz}/I_{zz}$, where I_{yz} and I_{zz} denote the integral intensity of the 647 cm^{-1} band for the $x(yz)x$ and $x(zz)x$ polarizations, respectively. In order to get more insight into the behaviour of $K_3Nb_3O_6(BO_3)_2$, we have performed additional IR studies (for experimental reasons these studies were performed only below room temperature). The IR spectra do not show so clearly the onset of the phase transition at 185 K (see figure 2). However, some weak changes in frequency and relative intensity of bands can also be observed, especially for the 147, 625, and 695 cm^{-1} bands.

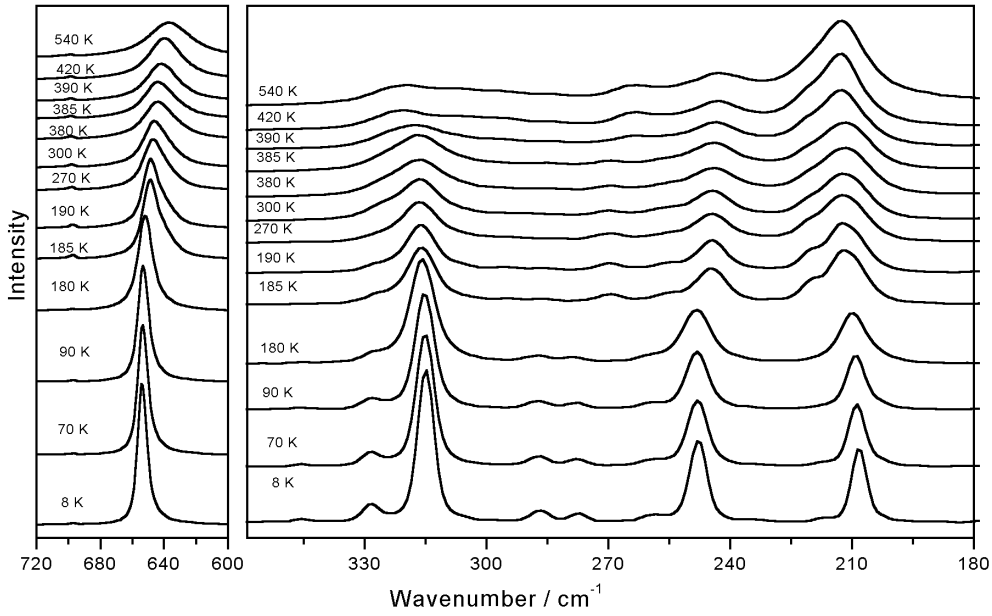

Figure 4. Temperature dependence of the most characteristic Raman spectra of $K_3Nb_3O_6(BO_3)_2$ measured in the polarization $x(zz)x$.

The main changes observed in the spectra can be followed by analysing the frequency ω versus temperature T plot shown in figure 6 for the Raman-active modes (the temperature dependence of the IR modes is not shown since the observed changes are much weaker than those observed in the Raman experiment). The results shown in figure 6 indicate clearly that the material experiences structural modification at about 385 and 185 K. They show also that nearly all high frequency modes (above 600 cm^{-1}) exhibit a normal softening with increasing temperature over the whole temperature range studied (except for the 697 cm^{-1} mode which shows hardening). On the other hand, many modes in the range 200–330 cm^{-1} and all modes observed below 200 cm^{-1} show appreciable hardening with increasing temperature. The phase transitions can also be clearly observed in the plot of Raman intensity versus T for the 316 cm^{-1} mode (see figure 7). We observe also that many bands exhibit a large bandwidth increase with increasing temperature. Figure 8 shows the full width at half-maximum (FWHM) versus T for the 1066, 647, and 316 cm^{-1} bands.

Let us now discuss the observed temperature dependence of the Raman bands. The first phase transition was observed in the present studies near 385 K, in good agreement with results reported in the literature (388 K [7, 8]). The x-ray structure of the phase stable above 385 K is not known. However, the domain structure suggests that although the crystal structure changes, its symmetry may also be described by the same $P2_1ma$ space group as was found for the room temperature modification [9]. Our results show that the number of observed modes does not change during this transition. This suggests that the unit cell above and below $T_c = 385$ K contains the same number of molecular units. The observed changes are abrupt, indicating that this transition has a first-order character. The most significant changes in frequency and relative intensity are observed for the 647 and 200–330 cm^{-1} modes, which have been assigned by us to stretching vibrations of the NbO_6 octahedra, and modes involving a significant contribution of bending and librational motions of the NbO_6 octahedra, respectively. On the other hand,

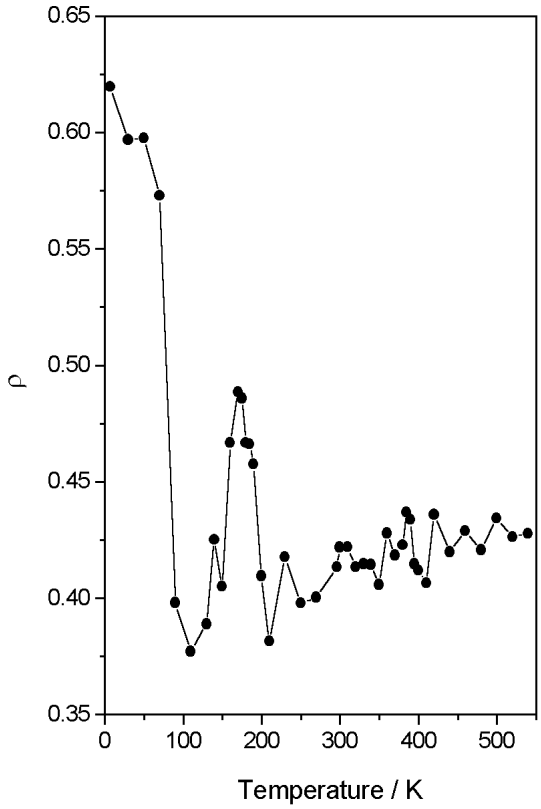

Figure 5. Depolarization ratio $\rho = I_{yz}/I_{zz}$ versus temperature for the 647 cm^{-1} mode.

no or very small changes could be seen for the bands below 200 cm^{-1}, assigned to T′(K^+) and T′(Nb^{6+}) modes, as well for the stretching modes of the BO_3^{3-} ions, observed at 1066 and 1200–1300 cm^{-1}. This result strongly suggests that the 385 K phase transition corresponds to tilts of the NbO_6 octahedra or/and displacement of Nb within the NbO_6 group. However, the observed frequency jumps do not exceed 10 cm^{-1}, indicating that the Nb–O bond lengths are weakly affected by this transition. It is worth adding that ionic conductivity studies revealed that this transition is also associated with a jump increase of K^+ ion conductivity above T_c [8]. Former studies of superionic materials showed that such a jump increase of conductivity during heating leads often to a jump FWHM decrease at T_c for some bands due to decrease of the couplings with the surroundings [23, 24]. This decrease of coupling above T_c was attributed to increase of the effective charge of mobile ions [23]. The present studies of $K_3Nb_3O_6(BO_3)_2$, showing this kind of behaviour for the 316 cm^{-1} band (see figure 8), may indicate that above 385 K the effective charge of K^+ ions increases considerably. On the other hand, increase of the ionic conductivity with temperature is evidenced for superionic materials by a large damping increase of those modes which involve vibrations of atoms strongly interacting with mobile ions [23]. In our case large anharmonic damping is observed, for example, for the 647 and 1066 cm^{-1} modes (see figure 8). The strength of the third- and fourth-order anharmonicity can be analysed in terms of the phonon–phonon coupling presented as [25]

$$\Gamma(T) = \Gamma_0 + C\left(1 + \frac{2}{e^x - 1}\right) + D\left(1 + \frac{3}{e^y - 1} + \frac{3}{(e^x - 1)^2}\right) \quad (1)$$

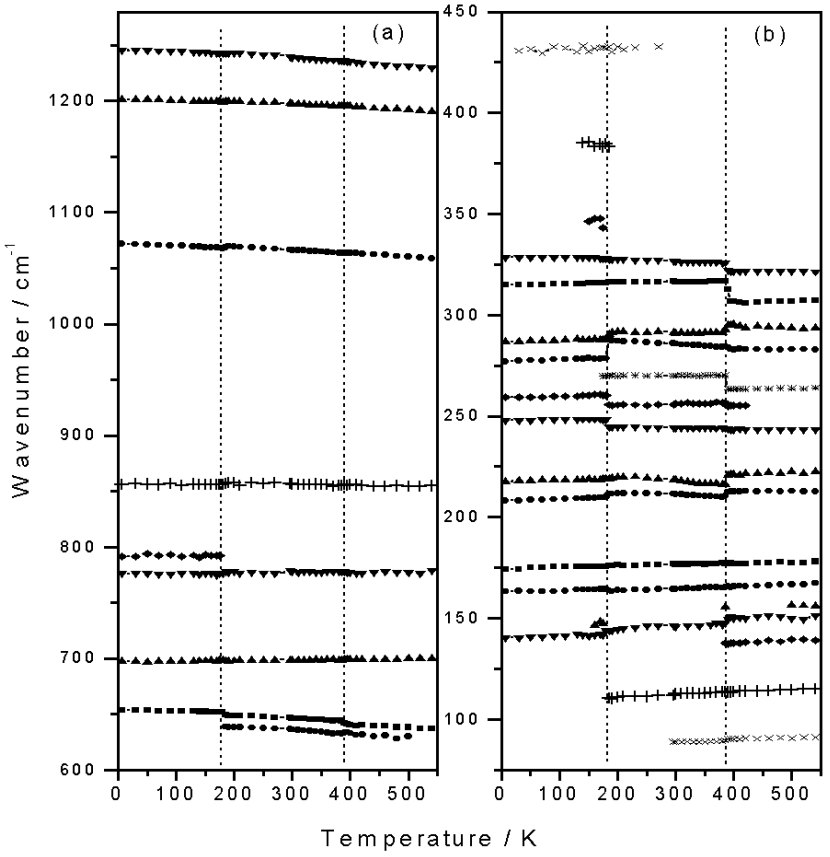

Figure 6. Mode frequencies of various Raman modes of $K_3Nb_3O_6(BO_3)_2$ as a function of temperature in the high frequency (a) and low frequency (b) ranges. The solid lines are to guide the eye.

where $x = h\omega_0/2k_BT$ and $y = h\omega_0/3k_BT$ refer to terms of three- and four-phonon decay processes. Γ_0 is due to broadening due to factors other than the anharmonic phonon decay, such as defects. At higher temperature the three- and four-phonon decay terms vary as T and T^2, respectively. Best fitting of the experimental data to the function of equation (1) is shown in figure 8. The values Γ_0, C, and D are 0.8, 2.1, and 2.6 for the 1066 cm^{-1} mode, 0.8, 4.2, and 2.2 for the 647 cm^{-1} mode, and 2.5, 1.8, and 0.15 for the 316 cm^{-1} mode. D values for the 1066 and 647 cm^{-1} modes are very large, much larger than usually observed for ionic crystals, indicating that the four-phonon process contribution to the broadening of these phonons is very large. Such large D values are observed for many superionic conductors [24, 26].

The second phase transition is observed in the present studies near 185 K. The previous dielectric studies suggested that there are two phase transitions at 188 and 176 K and that they are close to second order [7, 8]. It has also been speculated that the intermediate phase may be incommensurate [7]. Our results confirm the presence of only one phase transition and show that this is a first-order transition. The first-order character is clearly evidenced by jump changes in frequency of some modes. The most significant jumps are observed for the modes involving vibrations of the NbO_6 octahedra. This behaviour is very similar to the behaviour observed at 385 K, indicating that this transition is also associated with tilts of the NbO_6 octahedra or/and

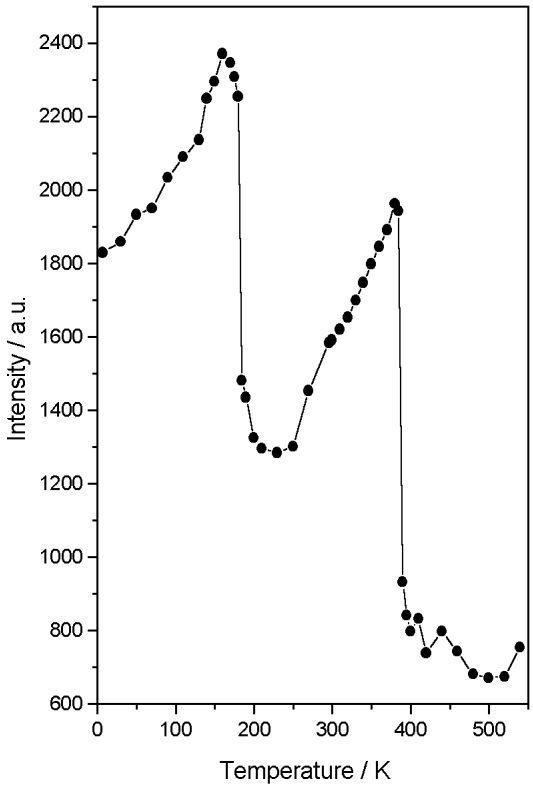

Figure 7. Intensity of the 316 cm^{-1} Raman-active modes as a function of temperature.

shifts of Nb atoms. Since there are no ionic conductivity reports for temperature below 300 K, it is not clear whether this transition is also associated with a jump increase in conductivity. The frequency changes are weaker than those observed at 385 K temperature. This indicates weaker changes in the crystal structure when compared to the changes occurring at 385 K. This result is consistent with the dielectric studies which showed that the low temperature dielectric anomaly is much weaker than the anomaly observed at 385 K [7].

As has already been mentioned, the behaviour of the depolarization ratio for the 647 cm^{-1} band suggests that this material may also exhibit a phase transition near 80 K. Similar jumps in depolarization ratio are also observed for other strong modes in the 320–200 cm^{-1} (not shown in figure 5). We observe also a few more weak changes at 80 K, which may indicate the onset of this transition, i.e. changes in slope of frequency versus temperature plots for the modes observed around 1200, 1240, and 176 cm^{-1}. The higher frequency modes show frequency increase with decreasing temperature to 80 K and no change below 80 K. The 176 cm^{-1} mode shows very weak temperature dependence in the 80–180 K range and a clear decrease below 80 K. Except for these changes, however, no frequency changes could be observed. Therefore, the confirmation of this transition requires further studies with other techniques.

Finally, our results show that a number of modes exhibit hardening with increasing temperature. It is known that the temperature dependence of the modes can be described by the following formula [27]:

$$[(1/\omega_j)(\mathrm{d}\omega_j/\mathrm{d}T)]_p = [(1/\omega_j)(\partial\omega_j/\partial T)]_v - \gamma_j\alpha \qquad (2)$$

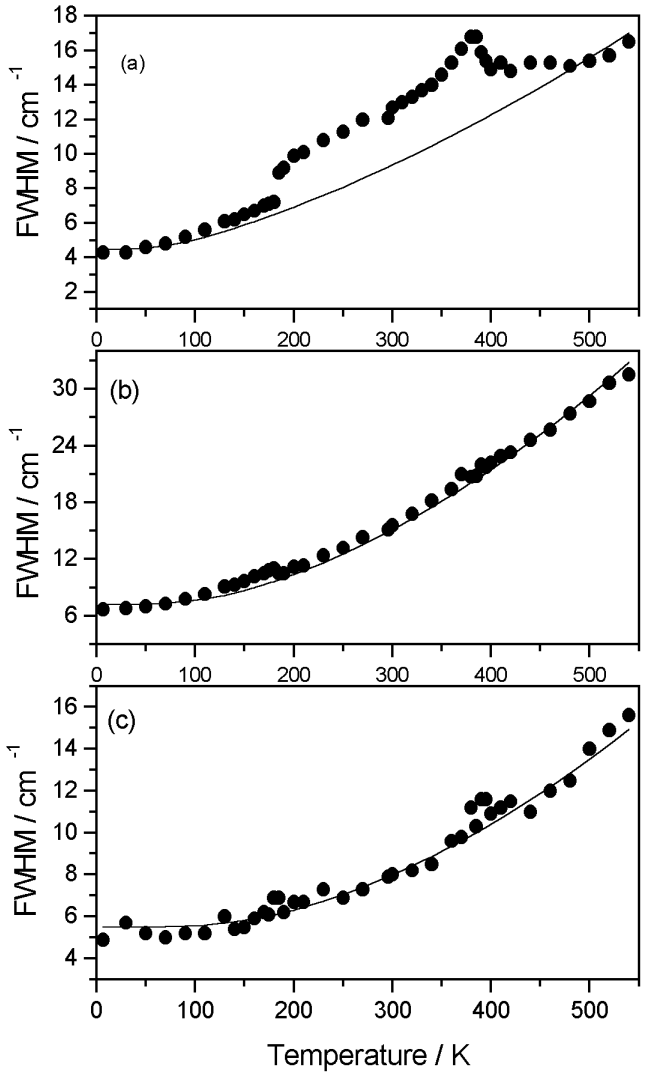

Figure 8. FWHM of the 316 (a), 647 (b), and 1066 cm^{-1} (c) modes. The solid curve is a least squares fitting of the experimental points to equation (1).

where $\gamma_j = -\partial \ln \omega_j / \partial \ln V = (B/\omega_j)(\partial \omega_j / \partial P)$ are mode Grüneisen parameters (B is the bulk modulus) and α is the thermal expansion coefficient. Since no data have been reported regarding the thermal expansion, bulk modulus, and pressure dependence of the frequencies, it is not possible to estimate the contributions of each of the terms on the right-hand side of equation (2) to the temperature dependence of the frequencies. It is worth noting, however, that positive frequency change with temperature is observed quite often. For example, it has been shown that the monoclinic phase of scandium molybdate, which exhibits positive thermal expansion, shows a frequency increase with increasing temperature for many modes due to the strongly positive 'true anharmonicity' (the first term in equation (2)) [27]. On the other hand, the orthorhombic phase of this material, exhibiting negative thermal expansion properties, exhibits a frequency decrease with increasing temperature.

4. Conclusions

The studies performed allowed us to an propose assignment of the observed modes to vibrations of NbO_6 and BO_3 groups as well as K^+ ions. They showed that the two phase transitions, observed near 385 and 185 K, are discontinuous and are associated with weak modification of the local environment of the Nb atoms within their oxygen octahedra as well as the local environment of the K^+ ions. The studies performed show that the four-phonon process contribution to the broadening of some modes is very large, similar to that observed for other superionic conductors. The present studies do not allow us to elucidate whether these transitions have displacive or an order–disorder character. These studies show also that this material may exhibit a phase transition around 80 K, not reported previously. However, the observed changes are weak and the confirmation of this transition needs further studies with other techniques.

References

[1] Kaminskii A A, Becker P, Bohaty L, Bagaev S N, Eichler H J, Ueda K, Hanuza J, Rhee H, Yoneda H, Takaichi K, Terashima I and Maczka M 2003 *Laser Phys.* **13** 1385
[2] Aka G, Kahn-Harari A, Mougel F, Vivien D, Salin F, Coquelin P, Colin P, Pelenc D and Damelet J P 1997 *J. Opt. Soc. Am.* B **14** 2238
[3] Nicholls J F H, Henderson B and Chai B H T 2001 *Opt. Mater.* **16** 453
[4] Hu X B, Wang J Y, Zhang C Q, Xu X G, Loong C K and Grimsditch M 2004 *Appl. Phys. Lett.* **85** 2241
[5] Becker P, Schneider J and Bohaty L 1993 *Z. Kristallogr. Suppl.* **S7** 14
[6] Becker P and Bohaty L 1995 *Z. Kristallogr. Suppl.* **S9** 28
[7] Voronkova V I, Kharitonova E P, Yanovskii V K, Stefanovich S Yu, Mosunov A V and Sorokina N I 2000 *Kristallografiya* **45** 888
[8] Kharitonova E P, Voronkova V I, Yanovskii V K and Stefanovich S Yu 2002 *Neorg. Mater.* **38** 978
[9] Kaminskii A A, Becker P, Bohaty L, Eichler H J, Penin A N, Ueda K, Hanuza J, Takaichi K and Rhee H 2004 *Phys. Status Solidi* a **201** 2154
[10] Becker P, Bohaty L and Schneider J 1997 *Kristallografiya* **42** 250
[11] Becker P, Held P and Bohaty L 1996 *Z. Kristallogr.* **211** 449
[12] Nakamoto K 1986 *Infrared and Raman Spectra of Inorganic and Coordination Compounds* (New York: Wiley)
[13] Xia H R, Li L X, Wang J Y, Yu W T and Yang P 1999 *J. Raman Spectrosc.* **30** 557
[14] Lorriaux-Rubbens A, Aka G, Antic-Findancev E, Keszler D A and Wallart F 2000 *J. Raman Spectrosc.* **31** 535
[15] Dominiak-Dzik G, Ryba-Romanowski W, Gołąb S, Macalik L, Hanuza J and Pajączkowska A 2000 *J. Mol. Struct.* **555** 213
[16] Mączka M, Tomaszewski P, Stępień-Damm J, Majchrowski A, Macalik L and Hanuza J 2004 *J. Solid State Chem.* **177** 3595
[17] Xia H R, Chen H C, Yu H, Wang K X and Zhao B Y 1998 *Phys. Status Solidi* b **210** 47
[18] Shen Z X, Hu Z P, Chong T C, Beh C Y, Tang S H and Kuok M H 1995 *Phys. Rev.* B **52** 3976
[19] Wang X B, Shen Z X, Hu Z P, Qin L, Tang S H and Kuok M H 1996 *J. Mol. Struct.* **385** 1
[20] Repelin Y, Husson E, Bennani F and Proust C 1999 *J. Phys. Chem. Solids* **60** 819
[21] De Andrés A, Agulló-Rueda F, Taboada S, Cascales C, Campá J, Ruiz-Valero G and Rasines I 1997 *J. Alloys Compounds* **250** 396
[22] Caciuc V, Postnikov A V and Borstel G 2000 *Phys. Rev.* B **61** 8806
[23] Wakamura K, Hirokawa K and Orita K 1996 *J. Phys. Chem. Solids* **57** 75
[24] Wakamura K, Miura F, Kojima A and Kanashiro T 1990 *Phys. Rev.* B **41** 2759
[25] Balkanski M, Wallis R F and Haro E 1983 *Phys. Rev.* B **28** 1928
[26] Wakamura K and Yoshida K 2003 *Solid State Ion.* **162/163** 7
[27] Ravindran T R, Sivasubramanian V and Arora A K 2005 *J. Phys.: Condens. Matter* **17** 277